

**Quantifying the effective attenuation length in high-energy photoemission experiments**

Maurizio Sacchi,<sup>1</sup> Francesco Offi,<sup>2</sup> Piero Torelli,<sup>1</sup> Andrea Fondacaro,<sup>2</sup> Carlo Spezzani,<sup>1</sup> Marco Cautero,<sup>3</sup> Giuseppe Cautero,<sup>3</sup> Simo Huotari,<sup>4</sup> Marco Grioni,<sup>5</sup> Renaud Delaunay,<sup>6</sup> Mauro Fabrizioli,<sup>7</sup> György Vankó,<sup>4</sup> Giulio Monaco,<sup>4</sup> Guido Paolicelli,<sup>2</sup> Giovanni Stefani,<sup>2</sup> and Giancarlo Panaccione<sup>7</sup>

<sup>1</sup>Laboratoire pour l'Utilisation du Rayonnement Electromagnétique, Centre Universitaire Paris-Sud, B.P. 34, F-91898 Orsay, France

<sup>2</sup>Istituto Nazionale per la Fisica della Materia and Dipartimento di Fisica, Università di Roma III, Via della Vasca Navale 84, I-00146 Roma, Italy

<sup>3</sup>Sincrotrone Trieste S.C.p.A., S.S. 14 Km 163.5, Area Science Park, I-34012 Trieste, Italy

<sup>4</sup>European Synchrotron Radiation Facility, B.P. 220, 38042 Grenoble, France

<sup>5</sup>Institut de Physique des Nanostructures, Ecole Polytechnique Fédérale de Lausanne, CH-1015 Lausanne, Switzerland

<sup>6</sup>Laboratoire de Chimie Physique—Matière et Rayonnement (UMR 7614), Université Pierre et Marie Curie, 11, rue P. et M. Curie, F-75231 Paris, France

<sup>7</sup>Laboratorio TASC, Istituto Nazionale per la Fisica della Materia, Area Science Park, S.S.14, Km 163.5, I-34012 Trieste, Italy

(Received 16 December 2004; published 26 April 2005)

We have determined the effective attenuation length of photoelectrons over the range of kinetic energies from 4 to 6 keV in Co, Cu, Ge, and Gd<sub>2</sub>O<sub>3</sub>. The intensity of the substrate (Si) and overlayer core level peaks was measured as a function of the thickness of the wedge-shaped overlayers. Experimental values vary between 45–50 Å at 4 keV and 60–65 Å at 6 keV in Co, Cu, and Ge. Smaller values (30 Å to 50 Å, respectively) are found in Gd<sub>2</sub>O<sub>3</sub>. Our results confirm that, for different classes of materials, high energy photoemission spectroscopy has the necessary depth sensitivity to go beyond surface analysis, yielding important information on the electronic properties of the bulk and of buried layers and interfaces.

DOI: 10.1103/PhysRevB.71.155117

PACS number(s): 79.60.–i

**I. INTRODUCTION**

Photoemission (PE) electron spectroscopy is one of the most powerful tools available for the investigation of the electronic properties of matter. Its strong surface sensitivity is fully exploited for studying the topmost atomic layers of a solid. Quantifying depth sensitivity<sup>1</sup> in PE experiments has been an ongoing subject of research for more than 30 years, generating a wealth of experimental and theoretical results (see, for instance, Refs. 2–4). Such studies are important not only to PE spectroscopy, but also to quantitative LEED analysis<sup>5</sup> and electron energy loss spectroscopy.<sup>6</sup> It is relevant to the following discussion to point out that so far research has concentrated almost entirely on a range of electron kinetic energies ( $E_k$ ) that goes from a few tens of eV up to at most 2 keV, i.e., the range that is normally analyzed in PE experiments. At these kinetic energies, extreme surface sensitivity prevents PE spectroscopy from being used to investigate bulk electronic properties with negligibly small contributions from the surface. Important examples of this difficulty can be found in the analysis of strongly correlated systems, such as high temperature superconductors and heavy fermion systems.<sup>7</sup> From a more technologically oriented point of view, it is also important to stress the need for nondestructive methods of analysis capable of investigating the electronic properties of protected thin films, buried interfaces and multilayered devices.

In principle, the most straightforward way of increasing bulk sensitivity in PE experiments is to go towards higher values of  $E_k$  (4–10 keV). Hard x-ray photoemission spectroscopy (HAXPES) is very demanding in terms of photon flux, because of the low photoionization cross sections at high

photon energy.<sup>8</sup> This is one reason why there was no follow up to the pioneering experiments carried out on first generation synchrotron sources.<sup>9</sup> Taking advantage of the improved performance of modern storage rings, several projects have been started over the last few years with the aim of measuring the volume electronic properties of solids via HAXPES.<sup>10–14</sup> In addition, high performance laboratory sources have been designed and developed recently for specific applications where energy resolution is of little concern.<sup>15</sup>

Our project VOLPE (VOLume PhotoEmission from solids) has the objective of obtaining bulk sensitive valence band PE spectra with good statistics and with energy resolution comparable to that of standard PE experiments carried out in surface sensitive mode.<sup>14</sup> The results of the commissioning of the electron analyzer indicate that photon energies around 6 keV offer a good compromise between attainable energy resolution, increased depth sensitivity and a reduced cross section for valence band PE.<sup>13</sup> In particular, we were able to measure the Co 2*p* core level emission of a Co film buried under a 120 Å thick capping layer, and a rough estimate of the effective attenuation length (EAL) was given ( $\lambda = 50 \pm 5$  Å at 5 keV). It is clear, though, that in order to set realistic conditions for the feasibility of future experiments and to move into applications of high energy valence band photoemission, a more accurate and quantitative knowledge of the depth sensitivity is required.

Model calculations estimating the depth sensitivity in this range of kinetic energies are scarce. We will refer to the work of Jablonski *et al.*<sup>16</sup> and Cumpson and Seah,<sup>17</sup> whose computer codes are available at the cited websites. From the experimental point of view, an early study by Flitsch and Raider<sup>18</sup> estimated a mean escape depth of about 55 Å at 3.5

keV in Si and SiO<sub>2</sub>. More recently, Dallera *et al.*<sup>19</sup> determined the EAL in GaAs to be  $\lambda=53$  Å at 6 keV.

In this paper, we present the result of a systematic work dedicated to quantifying the effective attenuation length of high energy (4–6 keV) electrons. The energy dependence of the EAL at several keV has not been investigated extensively, let alone its material dependence. Yet, from the experience gained at low kinetic energies,<sup>20</sup> it appears very important to compare, even at this early stage, values of  $\lambda$  for different types of materials.

The samples that we used in our investigation were two-component systems of the kind wedge-shaped overlayer-A grown on substrate B. This choice allowed us to monitor in a simple way the intensity of core level emissions of both materials as a function of the thickness of A (this is the so-called overlayer method<sup>3</sup>). The substrate was always silicon, while overlayers were chosen in such a way as to cover different classes of materials, namely noble metals (Cu), open 3*d* shell metals (Co), semiconductors (Ge) and an open 4*f* shell, strongly correlated oxides (Gd<sub>2</sub>O<sub>3</sub>).

## II. SAMPLE PREPARATION

Wedge samples of Co, Cu, and Gd<sub>2</sub>O<sub>3</sub> were prepared *ex situ*, using magnetron sputtering. The nominal thickness gradient was 10 Å/mm for all samples. The Co sample was capped by a 20 Å thick homogeneous layer of Cu, to prevent oxidation. Gd<sub>2</sub>O<sub>3</sub> was obtained by mixing 5% of oxygen to Ar during the deposition of Gd (partial pressures were  $5 \times 10^{-4}$  mbar of O<sub>2</sub> and  $9.5 \times 10^{-3}$  mbar of Ar). Deposition rates (in the 1–2 Å/s range) were monitored by a quartz balance prior to deposition. All Si substrates were cut from the same wafer. The thin (8–10 Å) passivation oxide layer was not removed, in order to limit the possible intermixing with deposited films. The presence of the oxide layer contributes weak Si<sup>4+</sup> components that are well separated in energy from the Si<sup>0</sup> main lines of the substrate. In addition, it introduces a constant attenuation factor for all Si<sup>0</sup> peaks, but, being a constant factor, this does not affect our analysis of the overlayer thickness dependence of normal emission spectra.

In order to avoid artifacts in the analysis of the photoemission intensity, we checked the thickness of our samples by measuring the angular dependent specular reflectivity as a function of the position along the wedge. Reflectivity measurements were carried out at the x-ray metrology beamline 6.3.2 of the Advanced Light Source at the Lawrence Berkeley National Laboratory.<sup>21</sup>

Figure 1 shows an example of reflectivity measurements at different positions along the Co wedge. Oscillations in the reflectivity as a function of the scattering angle originate from the interference between the waves scattered at the vacuum-film and at the film-substrate interfaces.<sup>22</sup> By matching the oscillation period of the reflectivity, the local overlayer thickness can be determined precisely.<sup>23</sup> The results of the reflectivity analysis agree well with nominal thickness values, except that the Co film displayed an unexpected kink at around midposition (see Fig. 2). This deviation from linearity was accounted for by interpolating experimental val-

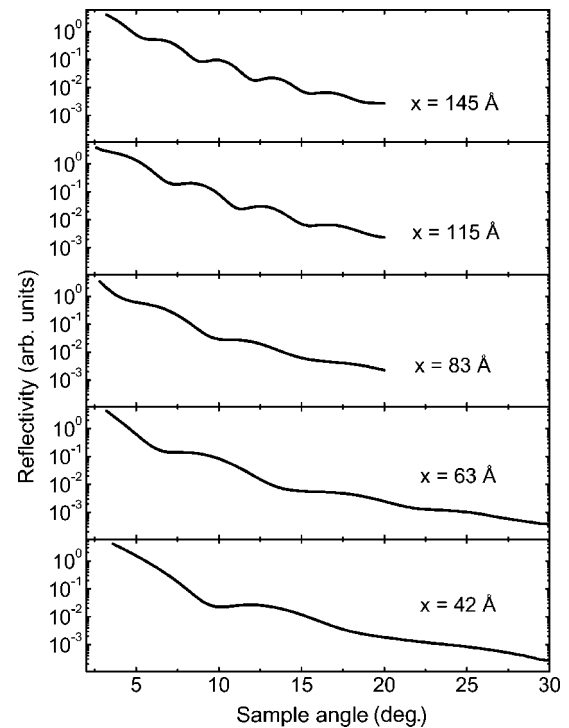


FIG. 1. Specular reflectivity curves measured at different positions on the Co wedge. The sample displacement is 2 mm between each successive curve. The photon energy is 777 eV. The estimated overlayer thickness  $x$ , indicated next to each curve, includes the Cu capping layer.

ues and by using the resulting thickness versus position curve in the analysis of photoemission data.

We also prepared four Ge samples, in the form of homogeneous films, by using an electron bombardment evaporator. Nominal (measured) thickness values were 25 (28) Å, 50 (48) Å, 75 (78) Å, and 100 (112) Å.

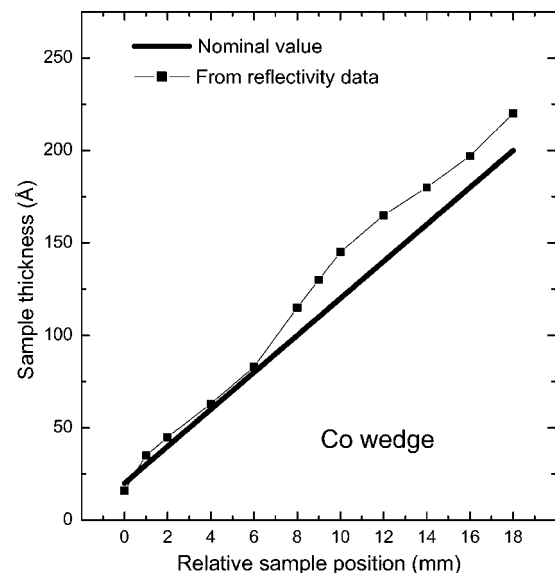


FIG. 2. A comparison between nominal and reflectivity-derived thickness values as a function of position along the Co wedge.

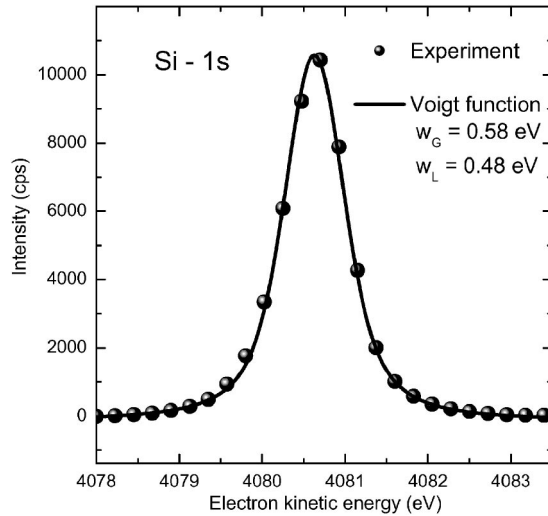


FIG. 3. Si-1s photoemission from the bare substrate, after subtraction of an integral background curve (dots). Experimental conditions are detailed in the text. The line is a Voigt function, assuming the nominal values of the experimental resolution (580 meV) and of the natural peak linewidth (480 meV).

### III. PHOTOEMISSION SETUP

High energy PE experiments were performed using the VOLPE analyzer. The complete setup was assembled at ESRF in January 2004 and installed on beamline ID16 for commissioning and first experiments. Results were very promising in terms of energy resolution: an overall bandwidth of  $\sim 70$  meV was attained at 6 keV, with equal contributions from the photon beam and from the analyzer.<sup>13</sup> Energy resolution, though, is not a major issue in the present experiment and, relaxing constraints on both the photon beam and the electron analyzer, we were able to measure core level spectra with good statistics also in the low current mode (30 mA on average) of the storage ring.

Using a combination of a Si(111) double crystal and a Si(220) channel cut for the monochromator, we obtained, at 6 keV, a flux of  $2 \times 10^{12}$  photons/second per 100 mA in the storage ring, with a photon energy resolution of 340 meV. The photon beam size at the sample position is  $60 \mu\text{m} \times 120 \mu\text{m}$  (FWHM vertical  $\times$  horizontal).

The electron analyzer was operated at a pass energy  $E_p$  of 60 eV, using an entrance slit of 1.6 mm. The spatial resolution of the two dimensional detector (0.1 mm/channel) defines the size of the exit slit. In the scan mode, we integrated the signal over 15 channels, for an effective exit slit of 1.5 mm. Under these conditions, the expected analyzer resolution is 470 meV, which, combined with the photon bandwidth, gives an overall resolution of 580 meV. Photoemission data confirm this estimate: Fig. 3 shows a Voigt fit to the 1s photoemission peak of Si, where the widths of the Gaussian and Lorentzian contributions are fixed to their nominal values of 580 meV and 480 meV,<sup>24</sup> respectively. The signal intensity is given in counts per second (cps), and such a spectrum could be collected in about 2 min.

The use of a position sensitive detector makes it possible to acquire spectra in the so-called fixed mode, i.e., accumu-

lating over the energy range defined by the acceptance of the detector in the dispersive direction, without changing any voltage. For a pass energy of 60 eV, this energy range is 4.5 eV, sufficient to record a whole photoemission peak (cf. Fig. 3). In our experiment we made use of this mode of acquisition, in addition to the standard step-by-step one.

### IV. DATA COLLECTION AND ANALYSIS

The thickness gradient axis in the wedge samples was oriented vertical, i.e., normal to the measurement plane defined by the incoming photons and by the collected electrons. In this way, we could select the overlayer thickness by a vertical translation of the sample, leaving the geometry of the PE measurement unaltered. All PE measurements were performed at room temperature, with the photon beam impinging at 45 deg onto the sample surface and by collecting photoelectrons at normal emission. We chose this experimental geometry in order to keep data analysis as simple as possible. It is now well recognized that the description of the emission depth distribution function (EDDF) as an exponential decay is not valid whenever elastic scattering events cannot be neglected.<sup>2-4</sup> On the other hand, making use of both numerical and analytical calculations, it was shown that the emission angle plays an important role in the shape of the EDDF function, and elastic scattering effects are enhanced at grazing emission.<sup>25</sup> At normal emission, the EDDF is well approximated by an exponential decay behavior and the EAL has a well defined value  $\lambda$  that can be obtained by a simple fit to the experimental data. Moreover, although rarely stated explicitly, model calculations taking into account the dependence on  $E_k$  indicate that elastic scattering effects on the EDDF become less important when going towards higher kinetic energies.<sup>5,26</sup> It should be stressed, though, that even under these favorable conditions  $\lambda$  should be regarded as a practical EAL value (as defined in Ref. 27) and, especially, that it should not be confused with the electron inelastic mean free path (IMFP),<sup>2,3</sup> which does not account for the influence of the elastic scattering processes.

We define  $\lambda$  as the thickness of the overlayer that reduces to 1/e the intensity  $I^s$  of a core level emission from the substrate, assuming a unitary intensity  $I_0^s$  for the bare substrate. Therefore, the intensity of a core level peak from the substrate varies as a function of the overlayer thickness  $x$  as

$$I^s(x) = I_0^s e^{-x/\lambda}.$$

In the same way, the intensity  $I$  of a peak related to the excitation of a core electron in the overlayer will vary as

$$I(x) = I_0(1 - e^{-x/\lambda}),$$

$I_0$  being the intensity for an infinite thickness of the overlayer. It is worth underlining that, in both cases,  $\lambda$  expresses a property of the overlayer material. Measuring the bare substrate and a very thick overlayer fixes the values of  $I_0^s$  and  $I_0$ , thus making  $\lambda$  the only free parameter for a given electron kinetic energy  $E_k$ .

Data were collected either in a scan mode or in a fixed mode. An example of the former is given in Fig. 4 for Co: whole PE spectra were recorded as a function of  $E_k$  at dif-

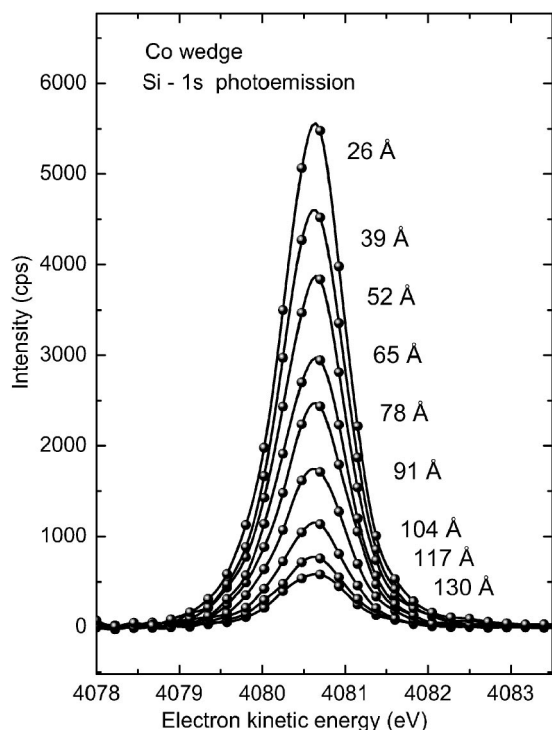


FIG. 4. Si-1s photoemission spectra as a function of the total overlayer thickness (values, in Å, are indicated next to each curve). All data are normalized to the incoming photon flux and on a counts-per-second basis. The accumulation time goes from 1 second per point for the thinnest overlayer to 6 seconds per point for the thickest one.

ferent sample positions, i.e., at different overlayer thickness values in the wedge. Raw data were corrected for photon flux and accumulation time. The area under the curve for the bare Si substrate was set to unity. To evaluate the EAL, these values were fitted with an exponential decay, yielding  $\lambda = 50 \pm 2$  Å (Fig. 5). The abscissa in Fig. 5 is the total overlayer thickness, i.e., we assumed that the 20 Å thick homogeneous capping layer of Cu behaves as Co (this was confirmed *a posteriori*). Alternatively, one can plot the intensity versus the actual Co thickness and scale the intensity of the bare silicon to account for the attenuation through 20 Å of Cu (using values in Table I). This procedure yielded  $\lambda = 51 \pm 2$  Å.

In the fixed mode, we set the kinetic energy of the analyzed peak at the center of the detector and, by scanning the sample height, we recorded the total peak intensity versus layer thickness. Another scan at 10 eV higher kinetic energy was also recorded to take into account variations in the background. The difference between the two measurements gave the variation of the peak area as a function of the overlayer thickness. Figure 6 shows three curves obtained in a fixed mode, measuring the Si-1s emission intensity as a function of the thickness of the Gd<sub>2</sub>O<sub>3</sub> overlayer. The sample was moved in steps of 0.2 mm, corresponding to a Gd<sub>2</sub>O<sub>3</sub> thickness variation of roughly 2 Å from one point to the next. The three curves differ for the photon energy employed (5925 eV, 7500 eV, and 8000 eV), hence for the kinetic energy of the photoelectrons. Lines are exponential best fits. The results

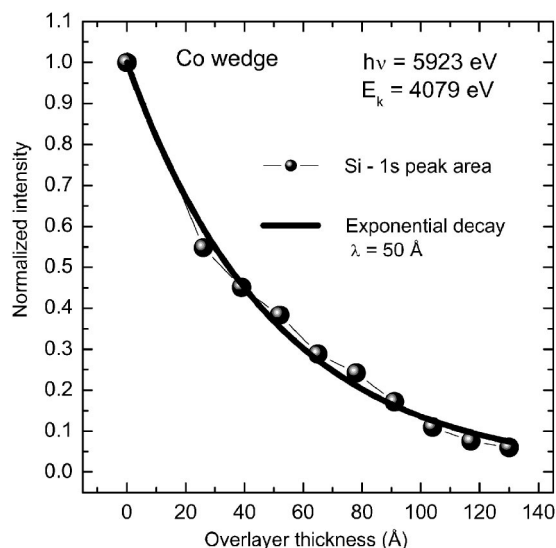


FIG. 5. The area of the curves in Fig. 4 after normalization to bare silicon (dots). The abscissa is the total overlayer thickness, including the 20 Å Cu capping layer. The continuous line is the best fit with an exponential decay function.

obtained using the two collection modes always agreed well. The fixed mode allows for faster data acquisition.

The results of our analysis are summarized in Table I, where  $\lambda$  values are given for different materials and different core level peaks. In Table I, we use the notation scan and fixed to refer to results obtained according to the two experimental procedures described above. The corresponding  $\lambda(E_k)$  values are shown in Fig. 7.

### V. DISCUSSION

Figure 7 gives an experimental estimate of the EAL in different materials for electron kinetic energies between 4 keV and 6 keV. The values that we obtain for Co, Cu, and Ge are fairly similar and close to predictions based on the best available models.<sup>16,17</sup> The full line in Fig. 7 is the IMFP in metallic Cu, as obtained using the NIST computer code.<sup>16</sup> Under our experimental conditions, one expects the EAL to be smaller than the IMFP.<sup>2,3</sup> One also expects this difference to diminish with increasing  $E_k$  values,<sup>26</sup> but we have not found models that quantify this trend between 4 keV and 6 keV. The data in Fig. 7 may be interpreted as suggesting that the difference between EAL and IMFP becomes smaller than the experimental error bar at high kinetic energies. On the other hand, in view of the discussion relative to Gd<sub>2</sub>O<sub>3</sub> data below, we believe that such a conclusion cannot be drawn on a firm basis yet.

A quantitative comparison with other experimental data on similar materials can be made with the results obtained recently by Dallera *et al.*,<sup>19</sup> who analyzed three GaAs samples where an AlAs layer of given thickness was introduced at various depths (20, 40, and 60 Å from the surface). They determined  $\lambda(E_k)$  values of 44 Å at 4450 eV and of 53 Å at 6050 eV, with an  $(E_k)^{0.5}$  dependence over the 800–6000 eV range of kinetic energies. Our results for Co, Cu, and Ge



TABLE I. Summary of the experimental results. From left to right, columns contain (i) overlayer material; (ii) photon energy; (iii) core level used for the analysis; (iv) type of measurement (either independent spectra or fixed mode acquisition); (v) electron kinetic energy; (vi) value of  $\lambda$  and corresponding error bar estimated from an exponential fit to the data; (vii) calculated  $\lambda_{\text{IMFP}}$  values from Refs. 17 and 30 (values in parentheses are from Ref. 16).

Layer	$\hbar\omega$ (eV)	Core level	Data type	$E_k$ (eV)	$\lambda$ (Å)	$\lambda_{\text{IMFP}}$ (Å)
Co	5925	Si 1s	Scan	4079	50±2	40
	"	Si 1s	Fixed	4079	51±2	41
	"	Co 2p	Fixed	5140	55±2	49
	"	Si 2s	Scan	5769	61±3	54
	"	Si 2s	Fixed	5769	60±3	54
Cu	"	Si 1s	Fixed	4079	44±4	40 (50)
	"	Si 2s	Scan	5769	62±6	54 (67)
Ge	"	Si 1s	Scan	4079	47±3	52 (51)
	"	Ge 3s	Scan	5738	65±6	69
Gd <sub>2</sub> O <sub>3</sub>	"	Si 1s	Scan	4079	31±1	51
	"	Si 1s	Fixed	4079	31±3	51
	"	Gd 3p	Scan	4372	32±3	54
	"	Gd 3p	Fixed	4372	34±4	54
	7500	Si 1s	Fixed	5654	43±4	67
	5925	Gd 4d	Scan	5765	44±5	68
	"	Gd 4d	Fixed	5765	46±6	68
	"	Si 2p	Scan	5818	44±4	69
	"	Si 2p	Fixed	5818	45±5	69
	8000	Si 1s	Fixed	6154	51±3	72

give larger values of  $\lambda$  (44–51 Å at 4079 eV and 60–65 Å at 5738 eV). These are not major differences and agreement may be regarded as moderately good insofar as a clear trend is demonstrated.

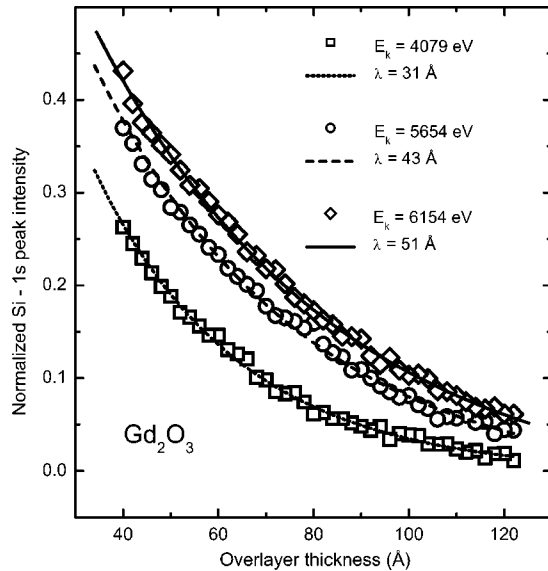


FIG. 6. Sample scans in fixed mode acquisition (see the text). The normalized Si-1s peak intensity is plotted against the Gd<sub>2</sub>O<sub>3</sub> overlayer thickness for three different kinetic energies. Lines are obtained by fitting with an exponential decay function.

The kinetic energy dependence of  $\lambda$  cannot be deduced from our data alone. If we consider, together with our results, also lower energy values of the EAL that can be obtained from the literature (e.g., EAL values for Cu based on the analysis of experimental data over the range  $E_k = 500$ – $1000$  eV<sup>28</sup>), a  $(E_k)^{0.75}$  behavior gives a fair fit to the ensemble of the data. On the one hand, such a behavior is at variance with the results of Dallera *et al.*,<sup>19</sup> based on the analysis of a single set of data extending over a wider energy range. On the other hand,  $(E_k)^{0.75}$  behavior is supported by recent calculations for both positrons and electrons up to 40 keV.<sup>29</sup>

Turning now to Gd<sub>2</sub>O<sub>3</sub>, the values that we obtain for  $\lambda$  are always smaller than for all the other samples. To check for spurious effects and experimental artifacts, we measured more points for Gd<sub>2</sub>O<sub>3</sub> (more emission lines and several photon energies) and obtained consistent results. The Gd<sub>2</sub>O<sub>3</sub> parameters relevant to the determination of the IMFP (density, energy gap, and number of valence electrons), lead to theoretical  $\lambda_{\text{IMFP}}$  values slightly larger than for Co or Cu. At this stage, we have no explanation for this discrepancy. A reduction factor of about 0.6–0.7 would be required to explain the difference between the calculated IMFP and the experimental EAL. Such a strong reduction is hardly encountered even at very low kinetic energies and this argument would not explain the difference between Gd<sub>2</sub>O<sub>3</sub> and the other samples. A theoretical evaluation of the IMFP in lanthanides has been the subject of debate and of changing points of view over the last few years, as illustrated, for instance, by the works of

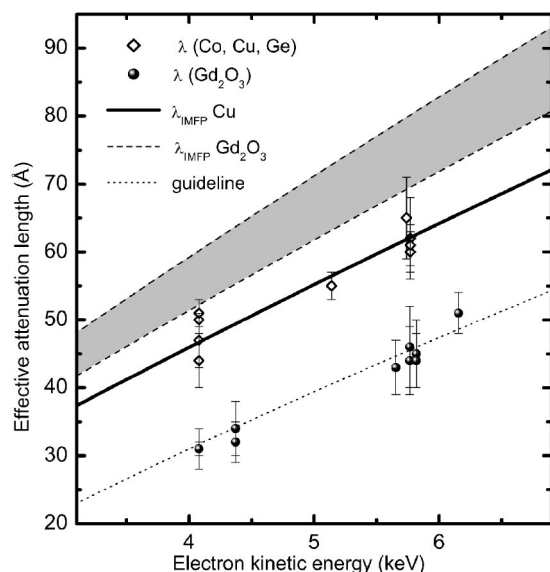


FIG. 7. A graph of the values  $\lambda(E_k)$  reported in Table I. Open diamonds represent experimental values for Co, Cu, and Ge, and filled circles those for  $\text{Gd}_2\text{O}_3$ . The full line is a calculation of  $\lambda(E_k)$  for Cu (Ref. 16). The two dashed lines and the encompassed gray area correspond to calculated values for  $\text{Gd}_2\text{O}_3$ , allowing for the maximum variation of parameters (Refs. 30 and 31). The thin dotted line is a guide for the eye, obtained by fitting  $\text{Gd}_2\text{O}_3$  data with a  $(E_k)^{0.75}$  dependence.

Seah *et al.*<sup>30</sup> and of Tanuma *et al.*<sup>31</sup> To appreciate the influence of different choices of parameters on calculated  $\lambda_{\text{IMFP}}$  values, we used the expression for the IMFP that is given in Ref. 31: varying every parameter within physically acceptable limits, we obtained values that are always within the shaded area in Fig. 7 and we were not able to reproduce our experimental results. Rare earths are known to have a peculiar behavior in terms of the electron mean free path at very low kinetic energies.<sup>20</sup> One would think, though, that the mechanisms invoked at low energy (mainly the high probability of exciting localized transitions of the  $4f$  electrons) are not very effective at several keV, and do not serve to explain our findings. Therefore, it remains an intriguing experimental observation that requires better understanding and modeling.

Overall, our results confirm that, for  $E_k \sim 6$  keV, photoelectrons can travel an average distance of 50 to 65 Å before suffering an inelastic collision. The corresponding information depth (defined as the layer thickness from which 95% of the total signal is produced<sup>2,3</sup>) is of the order of 150–200 Å. This is in agreement with earlier measurements of thin films buried under more than 100 Å thick overlayers.<sup>13,19</sup>

These values have two implications.

(i) Surface contributions at 6 keV are of the order of 2 to 7% of the total intensity (Fig. 8), according to the thickness of the surface layer being taken as 1 or 5 Å, respectively. For comparison, when working at ten times lower kinetic energy (note that  $E_k = 600$  eV would be considered already as high energy photoemission by usual standards), the surface layer contributes 12% of the total intensity if it is 1 Å and 46% if it is 5 Å. The corresponding information depth is 24 Å. Be-

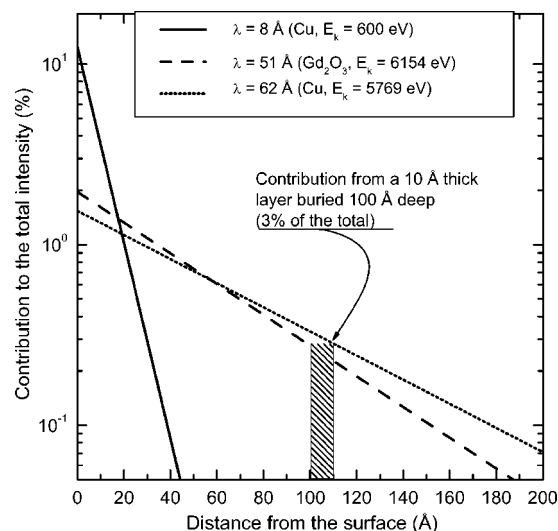


FIG. 8. The calculated contribution to the total intensity as a function of the distance from the surface. Dashed line:  $\sim 6000$  eV electrons in  $\text{Gd}_2\text{O}_3$  ( $\lambda = 51$  Å). Full line:  $\sim 6000$  eV electrons in Cu ( $\lambda = 62$  Å). For comparison, the dotted line corresponds to 600 eV electrons in Cu, with a practical EAL of 8 Å (Ref. 16).

ing able to put figures on these quantities is very important to support the idea that high energy photoemission is a bulk probe of the electronic properties of solids.

(ii) Typical capping layers which are used for protecting samples from contamination are 20 to 40 Å thick, and they will only reduce the signal from the underlying sample by less than a factor of 2. This implies that protected samples can be measured easily and that *in situ* preparation under ultrahigh vacuum conditions is no longer a strict requirement for core level photoemission spectroscopy. Also, the signal from buried interfaces and thin films will be more accessible. When  $\lambda$  is  $\sim 60$  Å, for instance, a film 10 Å thick buried under a 100 Å layer will still contribute a measurable fraction ( $\sim 3\%$ ) of its core level bulk signal (Fig. 8), while the corresponding intensity at 600 eV ( $3 \times 10^{-6}$ ) would not be detectable.

## VI. SUMMARY

We have measured the effective attenuation length  $\lambda$  of high energy photoelectrons in Co, Cu, Ge, and  $\text{Gd}_2\text{O}_3$ . Experimental values in Co, Cu, and Ge vary between 45–50 Å at 4 keV and 60–65 Å at 6 keV, in fair agreement with theoretical predictions.<sup>16,17</sup> At variance with calculations, smaller values (respectively, 30–35 Å and 45–50 Å) are found in  $\text{Gd}_2\text{O}_3$ . Overall, our results confirm that, for different classes of materials, high energy photoemission has the necessary probing depth to be considered a volume sensitive technique. Although these results do not exhaust the need for systematic characterization studies on different materials, they help us to define boundaries for the depth sensitivity of high energy photoemission experiments.

## ACKNOWLEDGMENTS

The authors thank Coryn F. Hague (LCP-MR, Paris) for helpful discussions and for his suggestions. Professor Yves

Baer contributed many ideas and provided continuous support to this project from its very beginning. This work received financial support from the European Community under RTD Contract No. HPRI-CT-2001-50032 and from the

Swiss OFES under Contract No. 02.0058. P. T., C.S., F. O., and A. F. acknowledge the European Community for granting their fellowships under contract No. HPRI-CT-2001-50032.

- <sup>1</sup>Over the years, diverse nomenclature has been used to describe the depth sensitivity of electron spectroscopies, which may be confusing. Throughout this paper, we have adopted the definitions of Powell *et al.* (Refs. 2–4) for the effective attenuation length (EAL)  $\lambda$ , the mean escape depth, the inelastic mean free path (IMFP)  $\lambda_{\text{IMFP}}$ , and the information depth, while terms like “depth sensitivity” or “probing depth” will be used with a loose and qualitative meaning.
- <sup>2</sup>C. J. Powell, A. Jablonski, I. S. Tilinin, S. Tanuma, and D. R. Penn, *J. Electron Spectrosc. Relat. Phenom.* **98–99**, 1 (1999).
- <sup>3</sup>A. Jablonski and C. J. Powell, *J. Electron Spectrosc. Relat. Phenom.* **100**, 137 (1999).
- <sup>4</sup>A. Jablonski and C. J. Powell, *Surf. Sci. Rep.* **47**, 33 (2002).
- <sup>5</sup>J. Rundgren, *Phys. Rev. B* **59**, 5106 (1999).
- <sup>6</sup>S. Tougaard and J. Kraer, *Phys. Rev. B* **43**, 1651 (1991).
- <sup>7</sup>L. Braicovich, N. B. Brookes, C. Dallera, M. Salvietti, and G. L. Olcese, *Phys. Rev. B* **56**, 15 047 (1997), and references therein.
- <sup>8</sup>J. J. Yeh and I. Lindau, *At. Data Nucl. Data Tables* **32**, 1 (1985).
- <sup>9</sup>I. Lindau, P. Pianetta, S. Doniach, and F. Spicer, *Nature (London)* **250**, 214 (1974).
- <sup>10</sup>A. Sekiyama and S. Suga, *J. Electron Spectrosc. Relat. Phenom.* **137–140**, 681 (2004); A. Sekiyama, S. Kasai, M. Tsunekawa, Y. Ishida, M. Sing, A. Irizawa, A. Yamasaki, S. Imada, T. Muro, Y. Saitoh, Y. Onuki, T. Kimura, Y. Tokura, and S. Suga, *Phys. Rev. B* **70**, 060506(R) (2004).
- <sup>11</sup>K. Kobayashi, M. Yabashi, Y. Takata, T. Tokushima, S. Shin, K. Tamasaku, D. Miwa, T. Ishikawa, H. Nohira, T. Hattori, Y. Sugita, O. Nakatsuka, A. Sakai, and S. Zaima, *Appl. Phys. Lett.* **83**, 1005 (2003); Y. Takata, K. Tamasaku, T. Tokushima, D. Miwa, S. Shin, T. Ishikawa, M. Yabashi, K. Kobayashi, J. J. Kim, T. Yao, T. Yamamoto, M. Arita, H. Namatame, and M. Taniguchi, *ibid.* **84**, 4310 (2004); A. Chainani, T. Yokoya, Y. Takata, K. Tamasaku, M. Taguchi, T. Shimojima, N. Kamakura, K. Horiba, S. Tsuda, S. Shin, D. Miwa, Y. Nishino, T. Ishikawa, M. Yabashi, K. Kobayashi, H. Namatame, M. Taniguchi, K. Takada, T. Sasaki, H. Sakurai, and E. Takayama-Muromachi, *Phys. Rev. B* **69**, 180508(R) (2004).
- <sup>12</sup>S. Thiess, C. Kunz, B. C. C. Cowie, T.-L. Lee, M. Renier, and J. Zegenhagen, *Solid State Commun.* **132**, 589 (2004).
- <sup>13</sup>P. Torelli, M. Sacchi, G. Cautero, M. Cautero, B. Krastanov, P. Lacovig, P. Pittana, R. Sergo, R. Tommasini, A. Fondacaro, F. Offi, G. Paolicelli, G. Stefani, M. Grioni, R. Verbeni, G. Monaco, and G. Panaccione, *Rev. Sci. Instrum.* **76**, 023909 (2005).
- <sup>14</sup>G. Paolicelli, G. Cautero, M. Cautero, A. Fondacaro, M. Grioni, P. Lacovig, B. Krastanov, G. Monaco, F. Offi, P. Pittana, M. Sacchi, R. Sergo, G. Stefani, R. Tommasini, P. Torelli, and G. Panaccione, *J. Electron Spectrosc. Relat. Phenom.* (to be published), available online at <http://dx.doi.org/10.1016/j.jespec.2005.01.114>
- <sup>15</sup>G. Beamson, S. R. Haines, N. Moslemzadeh, P. Tsakirooulos, P. Weightman, and J. F. Watts, *Surf. Interface Anal.* **36**, 275 (2004).
- <sup>16</sup>Calculated values of the IMFP up to 10 keV can be found, only for a few selected elements, at the NIST website <http://www.nist.gov/srd/nist71.htm>. See also C. J. Powell and A. Jablonski, *J. Phys. Chem. Ref. Data* **28**, 19 (1999); A. Jablonski, F. Salvat, and C. J. Powell NIST Electron Elastic-Scattering Cross Section Database, version 3.0, National Institute of Standards and Technology, 2002.
- <sup>17</sup>P. J. Cumpson and M. P. Seah, *Surf. Interface Anal.* **25**, 430 (1997); see also [http://www.lasurface.com/IMFP/Ag\\_IMFP\\_1.htm](http://www.lasurface.com/IMFP/Ag_IMFP_1.htm)
- <sup>18</sup>R. Flitsch and S. I. Raider, *J. Vac. Sci. Technol.* **12**, 305 (1975).
- <sup>19</sup>C. Dallera, L. Duò, G. Panaccione, G. Paolicelli, B. Cowie, J. Zegenhagen, and L. Braicovich, *Appl. Phys. Lett.* **85**, 4532 (2004).
- <sup>20</sup>Measurements performed on the low energy side of the so called *Universal curve of the electron mean free path in solids* show that EAL values depend strongly on the details of the electronic configuration of the sample. Large deviations are observed, for instance, for rare earths and *3d* transition metals [H. C. Siegmann, *J. Phys.: Condens. Matter* **4**, 8395 (1992)]. The analysis of the probing depth of x-ray absorption measurements performed in the total electron yield mode provides further evidence of these deviations [J. Vogel and M. Sacchi, *J. Electron Spectrosc. Relat. Phenom.* **67**, 181 (1994); R. Nakajima, J. Stöhr, and Y. U. Idzerda, *Phys. Rev. B* **59**, 6421 (1999); S. Gota, M. Gautier-Soyer, and M. Sacchi, *ibid.* **62**, 4187 (2000)].
- <sup>21</sup>J. H. Underwood, E. M. Gullikson, M. Koike, P. C. Batson, P. E. Denham, and R. Steele, *Rev. Sci. Instrum.* **67**, 3343 (1996).
- <sup>22</sup>See, for instance, M. Sacchi and A. Mirone, *Phys. Rev. B* **57**, 8408 (1998). Computer codes for calculating reflectivity in kinematic and dynamic theory are available at the websites [http://www.cxro.lbl.gov/optical\\_constants/multi2.html](http://www.cxro.lbl.gov/optical_constants/multi2.html) (by E. M. Gullikson) and [www.esrf.fr/computing/scientific/PPM/ppm.html](http://www.esrf.fr/computing/scientific/PPM/ppm.html) (by A. Mirone).
- <sup>23</sup>From reflectivity data, one obtains the mass thickness of the film (in  $\text{g}/\text{cm}^2$ ), which is also the relevant parameter for determining the EAL from photoemission data. For convenience, we will refer always to thickness values, assuming bulk densities for each of the analyzed materials.
- <sup>24</sup>M. O. Krause and J. H. Oliver, *J. Phys. Chem. Ref. Data* **8**, 329 (1979).
- <sup>25</sup>C. J. Powell and A. Jablonski, *J. Electron Spectrosc. Relat. Phenom.* **114–116**, 1139 (2001).
- <sup>26</sup>H. Shimada, N. Matsubayashi, M. Imamura, M. Suzuki, Y. Higashi, H. Ando, H. Takenaka, S. Kurosawa, S. Tanuma, and C. J. Powell, *Surf. Interface Anal.* **29**, 336 (2000).
- <sup>27</sup>A. Jablonski and C. J. Powell, *J. Alloys Compd.* **362**, 26 (2004).
- <sup>28</sup>Practical EAL values for Cu over the 500–1000 eV range were calculated using the computer code available at the

- NIST site (<http://www.nist.gov/srd/nist82.htm>), starting from the experimental results reported by B. Lesiak, A. Jablonski, J. Zemek, and P. Jiricek, *Surf. Interface Anal.* **26**, 400 (1998).
- <sup>29</sup>A. B. Denison and H. H. Farrell, *Phys. Rev. B* **69**, 104302 (2004).
- <sup>30</sup>M. P. Seah, I. S. Gilmore, S. J. Spencer, *J. Vac. Sci. Technol. A* **18**, 1083 (2000); M. P. Seah, I. S. Gilmore, and S. J. Spencer, *J. Electron Spectrosc. Relat. Phenom.* **120**, 93 (2001).
- <sup>31</sup>S. Tanuma, C. J. Powell, and D. R. Penn, *Surf. Interface Anal.* **35**, 268 (2003).